

Analysis of Dynamic Driving Control Systems (DDC) on a Full Vehicle Model in ADAMS

Dipl.-Ing. Alfred Pruckner

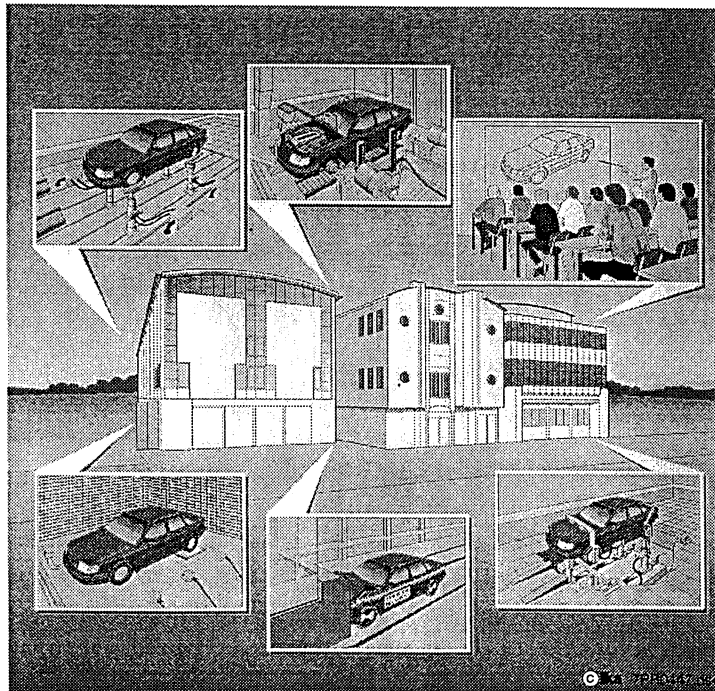
Dipl.-Ing. Michael Seemann

Institut für Kraftfahrwesen Aachen

RWTH Aachen

Steinbachstr. 10

52074 Aachen - Germany



1 Abstract

Beginning in 1978 with Antilock Brake Systems (ABS), more and more modern vehicles have been equipped with chassis management systems. Longitudinal slip control systems like ABS and Traction Control Systems (TCS) were used to control critical longitudinal driving situations. In addition to an optimum traction behaviour, lateral driving situations can be also improved by these systems because of larger lateral forces, possible on front and rear axle.

Beside pure longitudinal slip control systems, newest technology considers both longitudinal and lateral slip angles. These Dynamic Driving Control systems (DDC) monitor also lateral dynamic driving behaviour, and in contrast to longitudinal slip control systems, brake and engine management intervention may happen without the driver's activity.

This paper deals with the structure of Dynamic Driving Control systems. Checking system errors in a prototype vehicle is very dangerous and would be very expensive. To get a clear system knowledge under real test situations, many driving manoeuvres under the same and best environment conditions have to be done. For that reason multibody dynamic simulation programs like ADAMS are used to get general statements about the system's performance and failure behaviour.

For that purpose, a DDC algorithm, which controls the brake torque on each individual wheel, is added to an ADAMS full vehicle model. The control algorithm is divided into three subsystems: State identification, state observation and state control. The identification serves the driver's wanted state, observation serves the actual vehicle state and the control system compares these two states. Depending on identified understeering or oversteering driving situations, brake force is applied to the inner front wheel or the outer rear wheel.

Critical open and closed loop lane change manoeuvres on snow lanes which cannot be handled by the average driver, are used to analyse this lateral dynamic management system. Method and effect of DDC systems will be shown as well as different system errors like sensor offset or system failure during the management intervention.

2 Introduction

2.1 Dynamic Driving Control (DDC) systems

ABS and TCS can recognise critical longitudinal driving situations by the control of the longitudinal slip ratio. If at least one of the wheels starts to lock or spin, the controller will adjust the longitudinal slip ratio to the maximum possible longitudinal tire force (about 10% longitudinal slip ratio). However, maximum lateral vehicle stability will not be reached at this operating point, wherefore ABS and TCS cannot be used to optimise the vehicle's lateral driving behaviour [WAL95].

DDC supports the driver in critical lateral driving situations. If the vehicle enters a critical situation, the control algorithm will stabilise the vehicle by certain individual brake forces. The effect of DDC stabilising understeering and oversteering vehicle behaviour can be seen in the following Fig. 1.

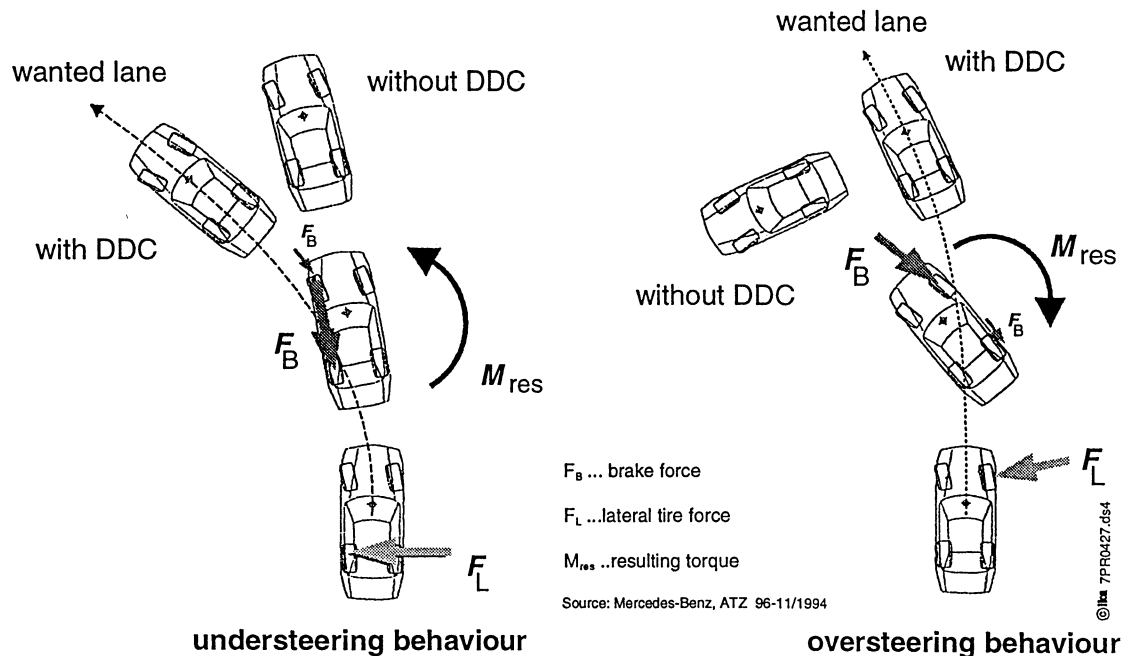


Fig. 1: Principal performance of DDC systems

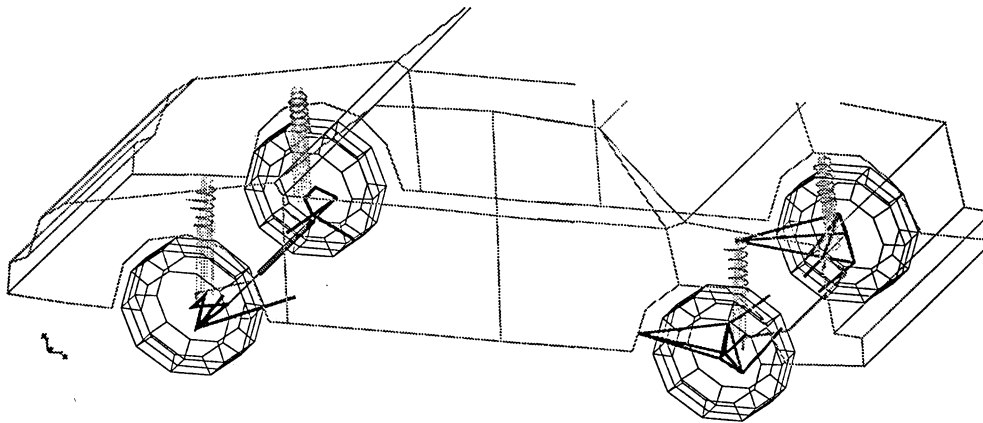
In case of understeering behaviour, main brake intervention happens on the inner rear wheel. Rear brake force causes a primary yaw torque and a reduction of the rear lateral tire force. Both effects help the vehicle's cornering.

In case of oversteering behaviour, main brake force on the outer front wheel helps to stabilise the vehicle. The intervention produces a primary yaw torque and reduces the lateral tire force at the front side. These effects prevent critical oversteering driving situations.

3 Modelling and software concept

3.1 Vehicle model

The vehicle model according to this presentation consists of 39 parts and 81 degrees of freedom. Fig. 2 presents the ADAMS vehicle and the rigid body model. The picture shows a McPherson suspension on the front and a multilink suspension at the rear side of the vehicle. Many connections are linked with bushing elements, the steering wheel input and drive train system are realised by coupler functions.



© Ika 7PR0421.ds4

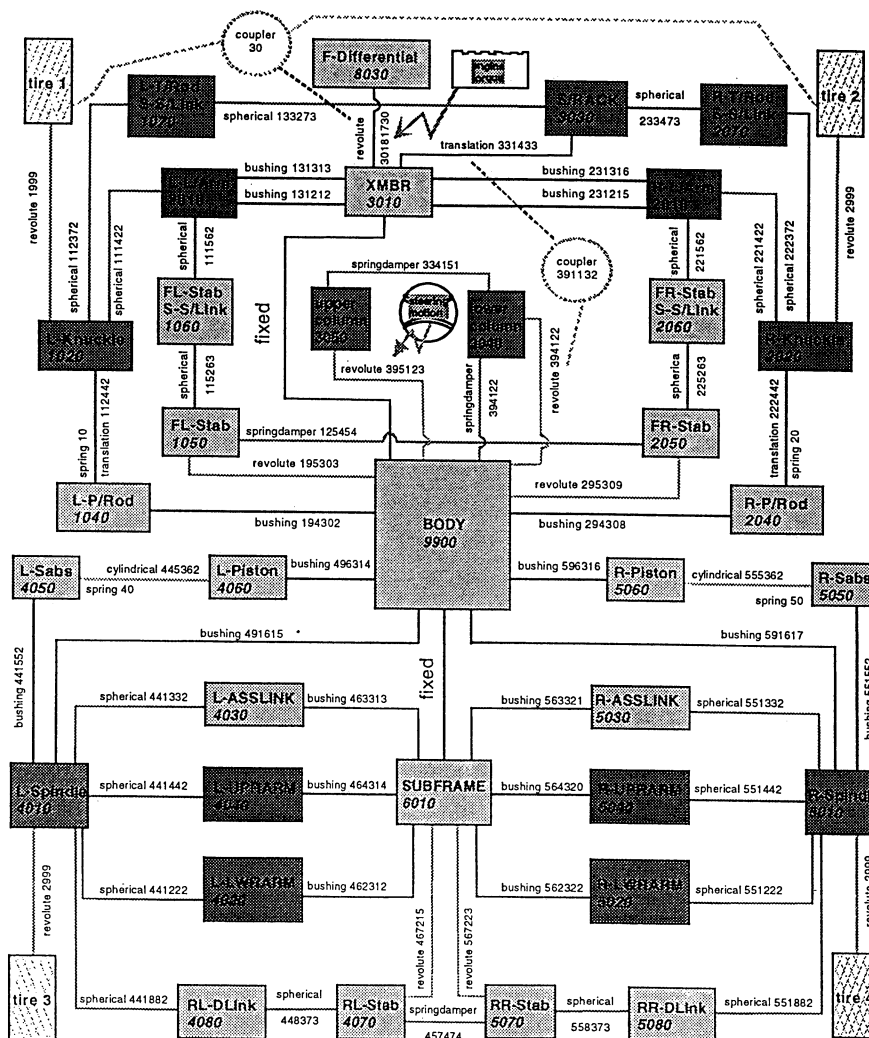


Fig. 2: ADAMS vehicle and rigid body model

3.2 Tire model

The ADAMS-tire model takes mutual longitudinal and lateral tire force influences into consideration. Fig. 3 shows longitudinal and lateral tire force characteristics with respect to the longitudinal slip ratio, respective lateral tire force and aligning torque characteristics with respect to side slip angle.

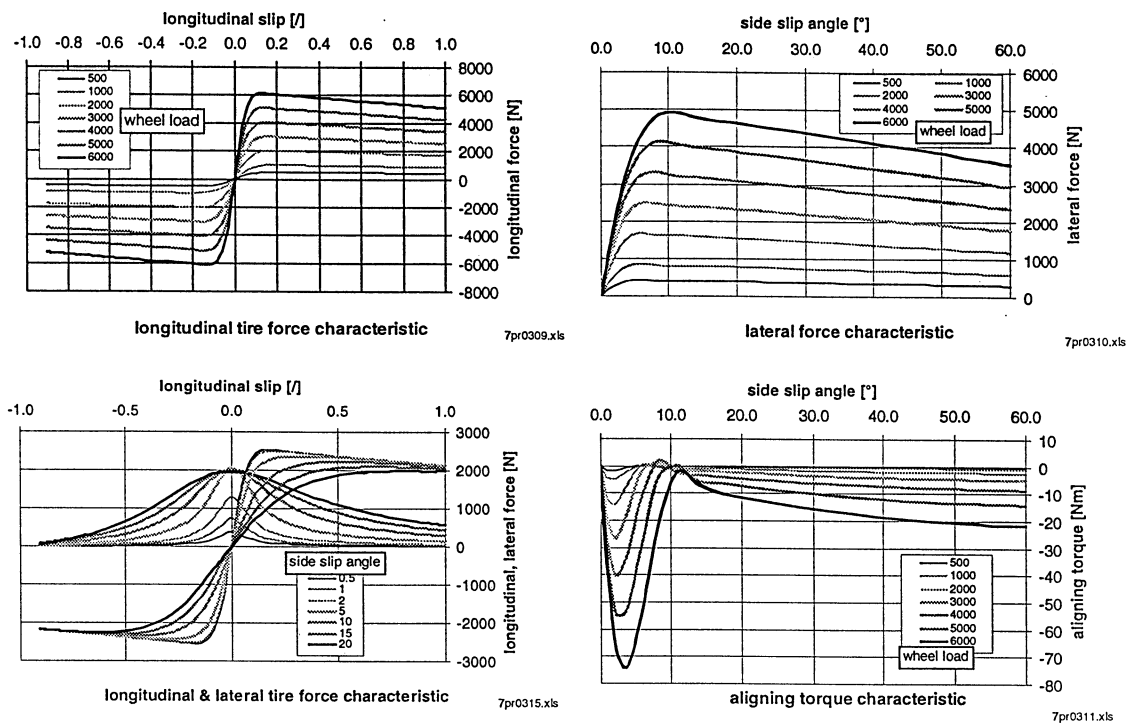


Fig. 3: ADAMS analytical tire model

3.3 Controller model

Some parts of the control algorithm are estimated directly in ADAMS (e.g. state identification). Others are modelled in the controller software MATRIXx and connected to ADAMS. The interface layout between ADAMS and MATRIXx can be seen in Fig. 4.

MATRIXx autocode generation delivers the control logic as a C-code file. With the additional use of a special template file, this generated C-code can be linked to ADAMS user written subroutines. The request-subroutine REQSUB manages the communication between ADAMS and controller software, the variable-subroutine VARSUB delivers the asked values to ADAMS. The digital rate between hardware simulation model (ADAMS, Fortran) and controller software (C-code) is determined in the ADAMS auto command file.

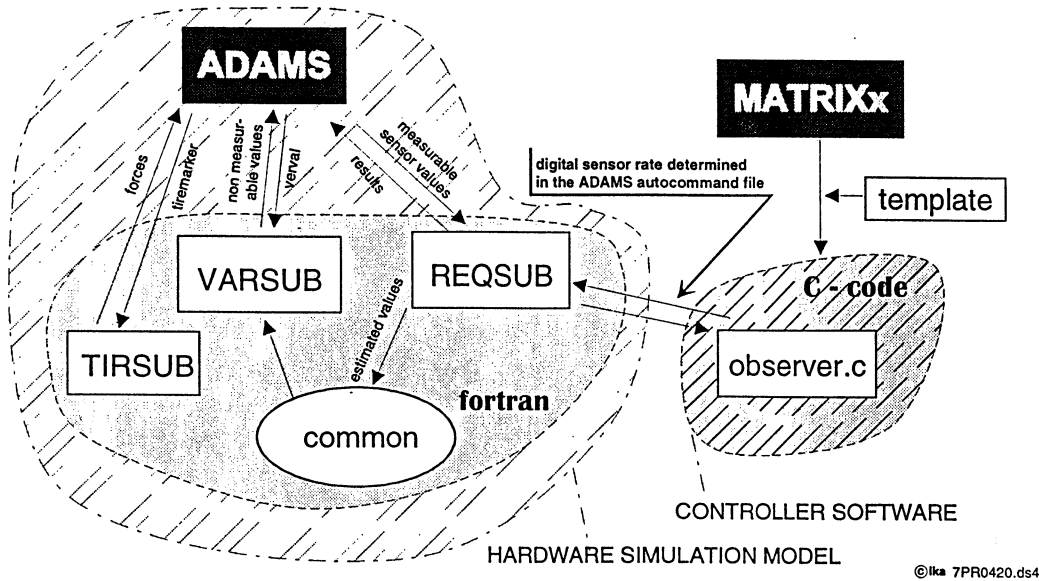


Fig. 4: Interface ADAMS - MATRIXx

The automatic generated C-code file can be placed in the controller environment of prototype vehicles later on.

3.4 DDC control algorithm

The DDC system presented in this paper will use both, yaw velocity and side slip angle, to control the lateral vehicle behaviour. Using only yaw velocity could cause wrongly identified vehicle state, the controller alone cannot prevent some critical driving situations clearly enough [ZAN96].

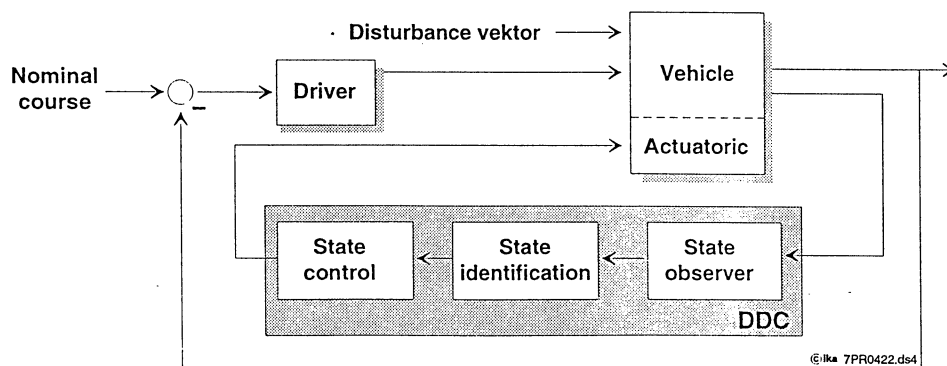


Fig. 5: DDC structure

Fig. 5 shows the principal structure of the used DDC system. The nominal course is adjusted by the driver (steering wheel, acceleration pedal). The vehicle follows the wanted lan.

dependent on the driver's ability and on external disturbances (e.g. wind forces, changing road conditions,...).

The control system is able to recognise, rate and control critical lateral driving situations. For that reason, the actual vehicle state (state observation) as well as the difference between actual and wanted lane (state identification) are determined as well as possible. Certain differences between wanted and real lane will be corrected by the state control system. This can be done independent of the driver's demand by activating individual brake and/or engine management interventions.

3.4.1 State observation

State observation has to deliver clear actual vehicle dynamic values by the use of right sensor systems. Non measurable values are determined by so-called observers. The principal structure of the vehicle state observer can be seen in Fig. 6.

The left side shows measurable sensor signals which are: all four wheel speeds, steering wheel angle, yaw velocity and longitudinal as well as lateral acceleration. The right side in this figure shows the values which will be delivered to the state identification system.

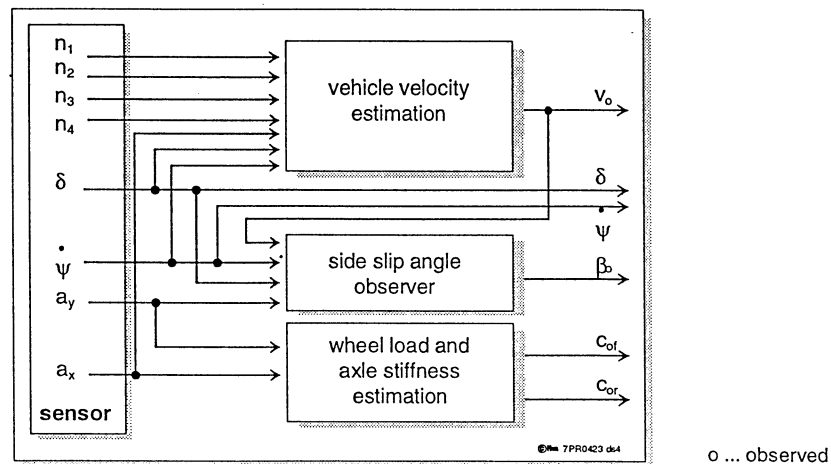


Fig. 6: Vehicle state observation

In consideration of yaw velocity, steering wheel angle and longitudinal acceleration the vehicle velocity is estimated by the analysis of all four wheel speeds. Furthermore, the actual wheel loads are determined with the help of measured longitudinal and lateral acceleration. These wheel loads are used to estimate the actual front and rear lateral axle stiffness.

The side slip angle is estimated by a so-called Kalman Filter [KOR94] which combines the measured steering wheel angle as well as lateral acceleration and yaw velocity with the estimated vehicle velocity. The principal structure of the Kalman filter can be seen in Fig. 7.

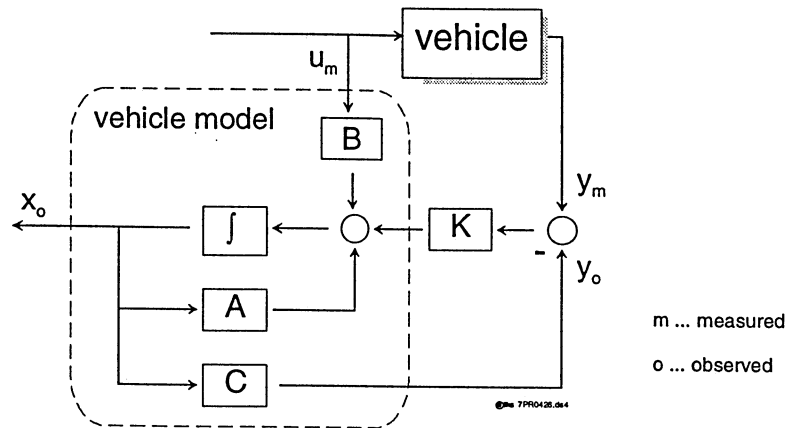


Fig. 7: Structure of the Kalman Filter

A two lane vehicle model is built up parallel to the vehicle and fed with certain, measurable input values u_m (e.g.: δ). Measurable output values from the vehicle (e.g.: a_y) are compared to the ones from the controller model ($y_m - y_o$), the difference is multiplied by the corrector matrix K and brought back into the two lane vehicle model. Estimated output values from the observer x_o (e.g.: β) are used as state identification system input.

3.4.2 State identification

Main task of state identification is the comparison between actual vehicle state and driver's demand. Based on the output values of the state observer the state identification algorithm has to decide whether the actual vehicle behaviour is in a critical situation. The identification of driver's demand is done by use of a dynamical single track vehicle model. Variable input values to this calculation are the steering wheel angle, vehicle velocity and actual axle stiffness', output values are wanted yaw velocity and wanted side slip angle. The next two formulas show the differential equation belonging to this estimation [RIC90, WAL96].

$$\ddot{\psi} + \left(\frac{c_{sv} + c_{sh}}{m \cdot v} + \frac{c_{sv} \cdot l_v^2 + c_{sh} \cdot l_h^2}{v \cdot \Theta_z} \right) \cdot \dot{\psi} + \left(\frac{c_{sh} \cdot l_h - c_{sv} \cdot l_v}{\Theta_z} + \frac{c_{sv} \cdot c_{sh} \cdot l^2}{m \cdot v^2 \cdot \Theta_z} \right) \cdot \psi = \left(\frac{c_{sv} \cdot c_{sh} \cdot l}{\Theta_z \cdot m \cdot v} \right) \cdot \delta + \frac{c_{sv} \cdot l_v}{\Theta_z} \cdot \dot{\delta} \quad (1)$$

$$\ddot{\beta} + \left(\frac{c_{sv} + c_{sh}}{m \cdot v} + \frac{c_{sv} \cdot l_v^2 + c_{sh} \cdot l_h^2}{v \cdot \Theta_z} \right) \cdot \dot{\beta} + \left(\frac{c_{sh} \cdot l_h - c_{sv} \cdot l_v}{\Theta_z} + \frac{c_{sv} \cdot c_{sh} \cdot l^2}{m \cdot v^2 \cdot \Theta_z} \right) \cdot \beta = \left(\frac{c_{sv} \cdot l_v}{\Theta_z} - \frac{c_{sv} \cdot c_{sh} \cdot (l_v \cdot l_h + l_h^2)}{m \cdot v^2 \cdot \Theta_z} \right) \cdot \dot{\delta} - \frac{c_{sv}}{m \cdot v} \cdot \delta \quad (2)$$

Because of variable input values to the controller, these calculations have to be done using 'DIFF' functions (instead of two TFSISO).

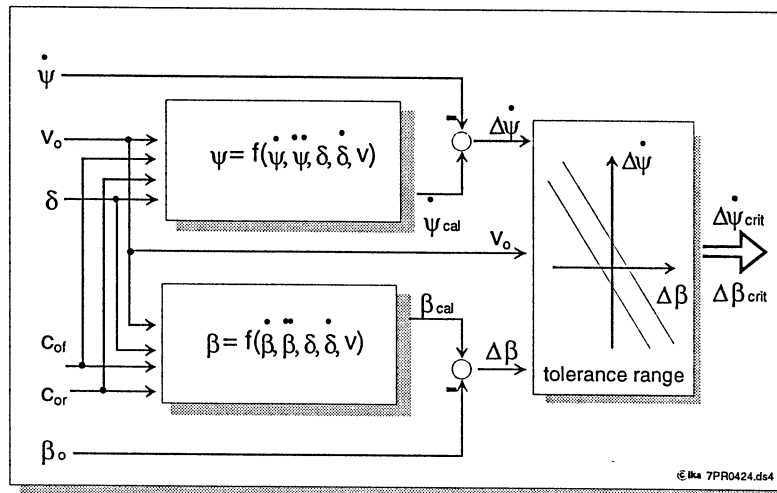


Fig. 8: Vehicle state identification

The identification whether there is understeering or oversteering vehicle behaviour is done by the control of the difference between wanted (calculated) and real (measured respectively observed) value of both space variables, yaw velocity and side slip angle (Fig. 8). These two differences are filtered by a well-defined, velocity dependent range of tolerance and transmitted to the state control system.

3.4.3 State control

The state controller algorithm (Fig. 9) uses a flat double track vehicle model with integrated HSRI tire model. This model is linearised about the actual working point during each calculation step. The controller is built up in MATRIXx and consists of two subsystems, Riccati controller and slip controller. The Riccati control algorithm estimates a certain matrix at each calculation step which has to be multiplied by the input vector. Two additional requirements can be formulated in this control algorithm.

The actual longitudinal slip ratios (λ_i), which have to be adjusted by the slip controller, will be delivered by this control algorithm [FÖL94]. The slip controller determines the wanted

individual brake pressures on each wheel (p_i). Further on, this slip controller can be used by longitudinal slip control systems like ABS and TCS, too.

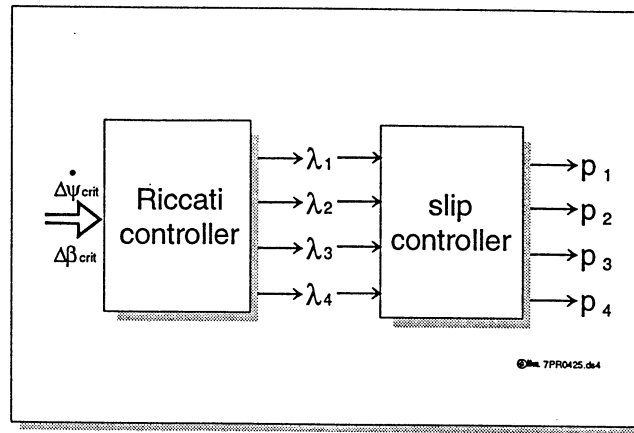


Fig. 9: Vehicle state control system

4 Simulation results

4.1 Open loop manoeuvre

Open loop driving manoeuvres are used for objective driving behaviour analysis. The vehicle inputs (steering angle, brake and acceleration request) are well defined, the vehicle response has no influence on these input values. The open loop simulation is done at 100 km/h, the steering angle according to the manoeuvre can be seen in the next Fig. 10.

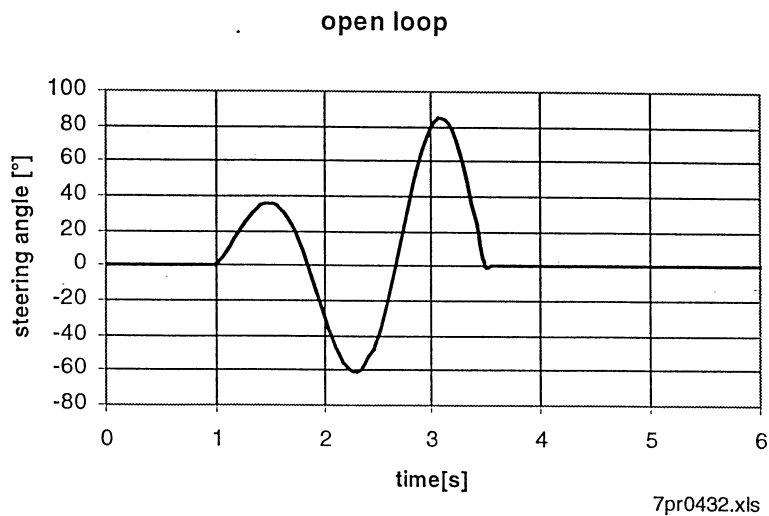


Fig. 10: Open loop manoeuvre, steering angle

The steering input equals three half sinus waves with increasing amplitude. Therefore, the vehicle response during the change from non-critical to critical behaviour can be studied. Steering angle and vehicle velocity together cause the vehicle response which can be seen in the next figures.

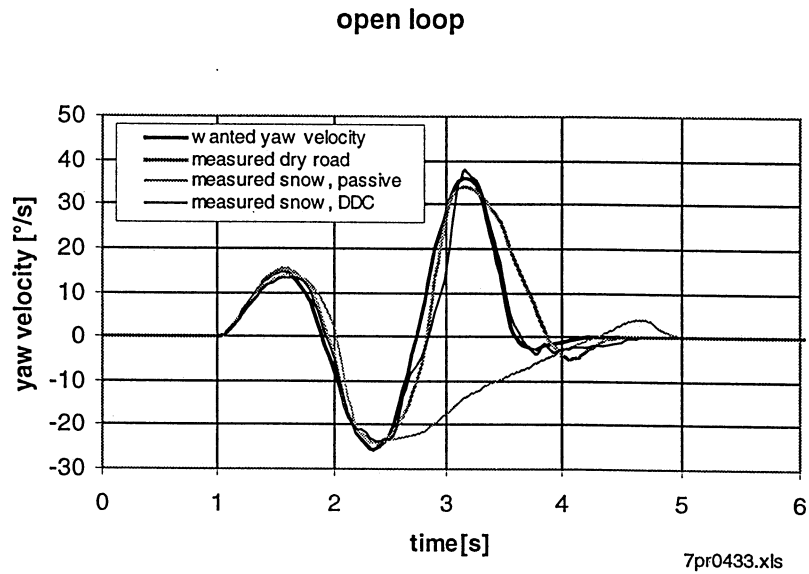


Fig. 11: Open loop manoeuvre, yaw velocity

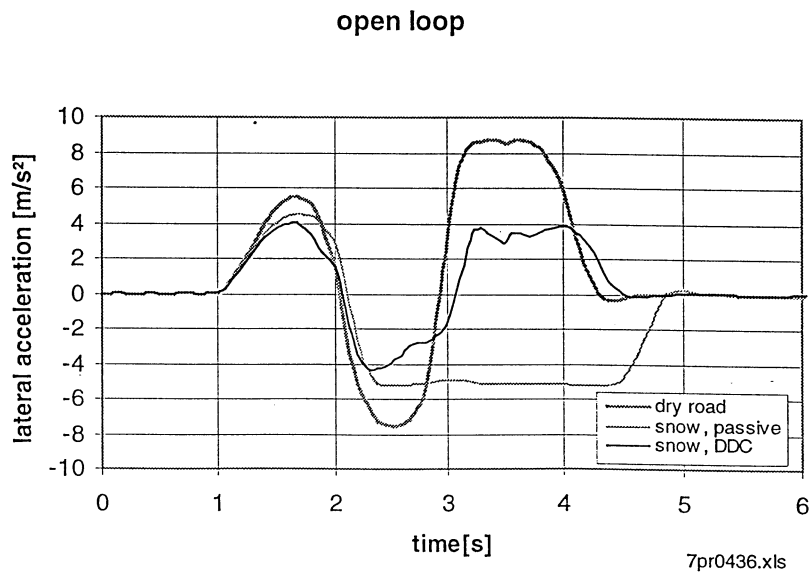


Fig. 12: Open loop manoeuvre, lateral acceleration

Fig. 11 shows the wanted yaw velocity determined by formula (1). The measured yaw velocity on dry road follows the wanted one well in the beginning and with some certain delay at the end of the manoeuvre. This is due to the fact that the lateral acceleration (Fig. 12) on dry road enters critical values ($\geq 6\text{m/s}^2$) in the second steering input wave. At this time the linear single track model (formula 1 and 2) cannot determine exactly the actual yaw velocity and side slip angle (Fig. 13).

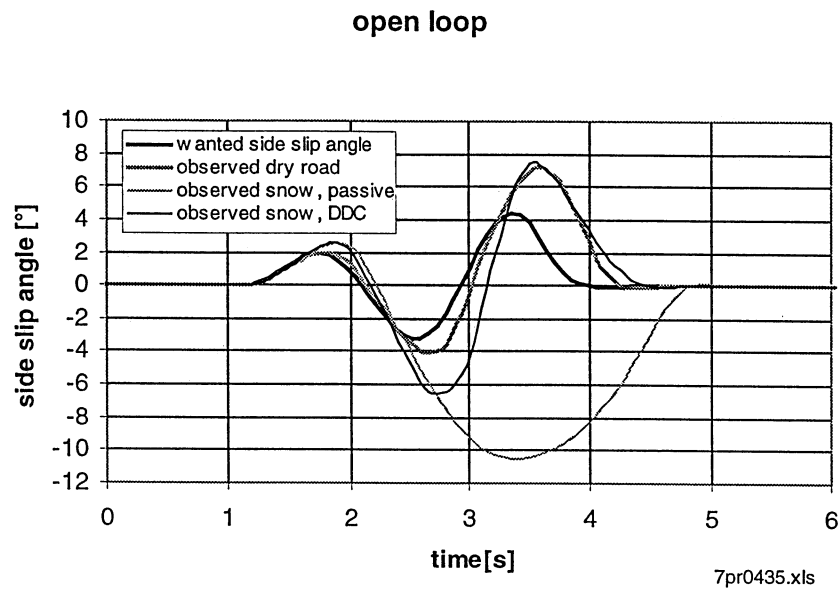


Fig. 13: Open loop manoeuvre, side slip angle

The passive vehicle behaviour on snow-covered road enters a critical situation after 2.5 seconds. The vehicle slides until the 5th second which can be seen by a constant lateral acceleration value and high side slip angles at this time. The vehicle on snow-covered lane which is controlled by the DDC system will follow the wanted yaw velocity as well as possible. The lateral acceleration will be adjusted to the maximum possible on snow-covered lane (4 m/s^2), the side slip angle will not reach values bigger than 8° .

In Fig. 14 the DDC brake intervention according to this open loop manoeuvre can be seen. Depending on oversteering or understeering behaviour, the brake torque is divided between front and rear side. Because this kind of manoeuvre produces understeering vehicle behaviour, the control algorithm asks for high lateral tire forces at the front side and low lateral tire forces on the rear side of the vehicle.

The longitudinal slip ratios on the rear axle will catch higher values than at the front axle. Fig. 15 shows the longitudinal slip ratios which are adjusted by the brake torque according to all 4 wheels.

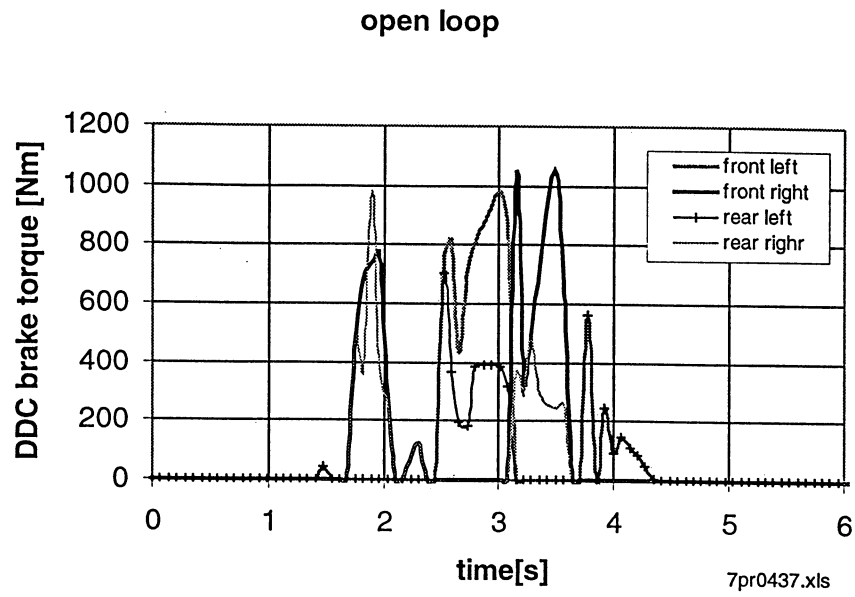


Fig. 14: Open loop manoeuvre, DDC brake intervention

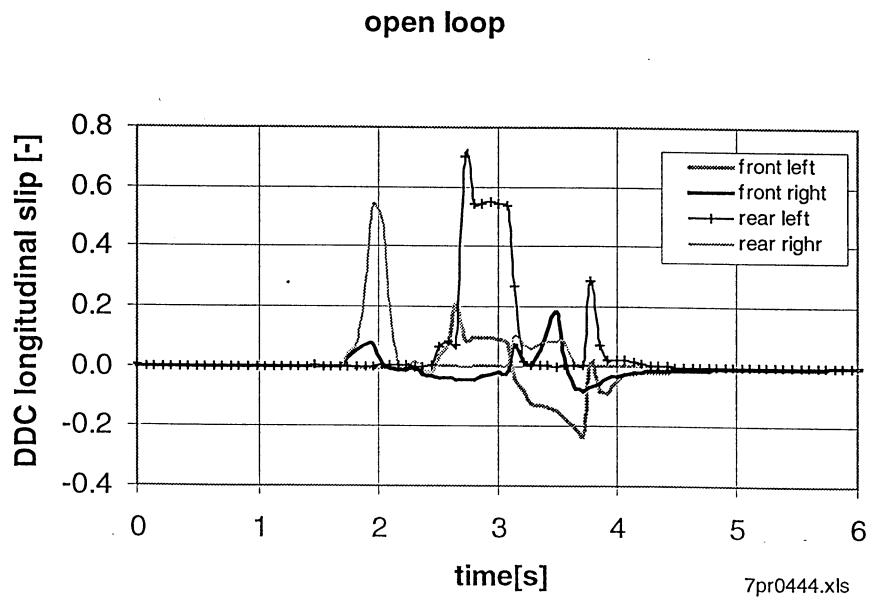


Fig. 15: Open loop manoeuvre, longitudinal slip ratios

4.2 Closed loop manoeuvre

In contrast to open loop driving manoeuvres closed loop driving manoeuvres will use the vehicle response to control the driving situation. Fig. 16 shows an ADAMS top view according to the closed loop double lane change manoeuvre at 80 km/h. The first manoeuvre is performed on dry road, the second one under icy road condition without controller and the third one under the same icy road conditions with DDC algorithm.

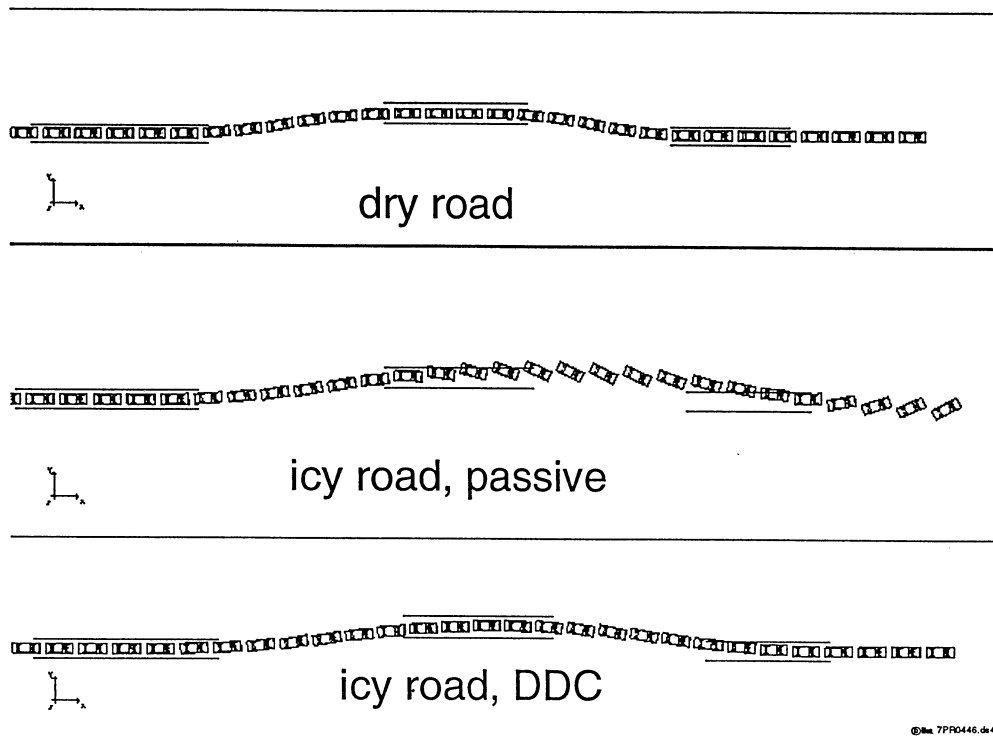


Fig. 16: Double lane change manoeuvre under dry respectively icy road conditions

The adjusted steering angle depends on the actual driving lane of the vehicle. Fig. 17 shows steering angle according to all three driving situations shown above.

Both manoeuvres, on dry road and on icy road with DDC, show the typical W-shape of successful double lane change manoeuvres. In contrast to these steering angles the passive vehicle on icy road shows typical critical steering angle values bigger than 90° .

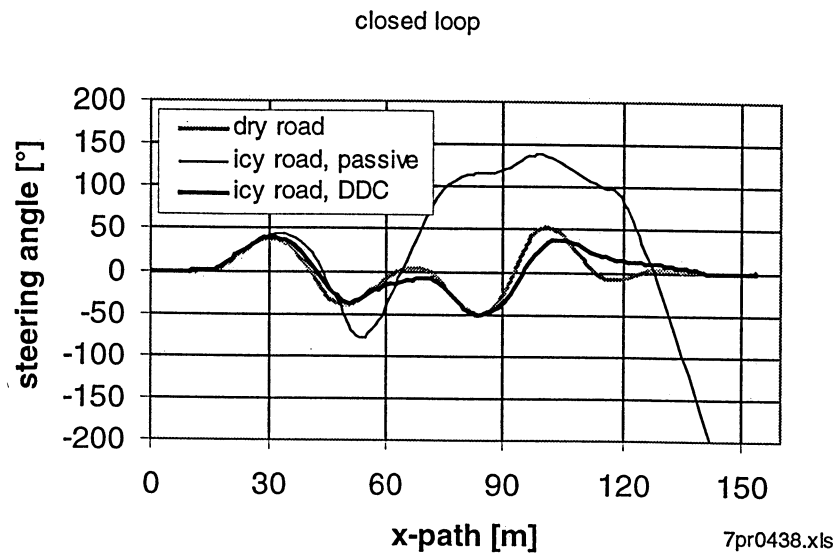


Fig. 17: Double lane change manoeuvre, steering angle

The x-y-lane (Fig. 18) cannot be followed exactly by the controlled vehicle on icy road, because the lateral acceleration (Fig. 19) reaches the physical limit (3m/s^2). But the result on icy road and controlled vehicle is much better than without controller. The controlled vehicle is able to return to the original lane about 20 meters later than on dry road. The vehicle without controller slides at this point of the manoeuvre.

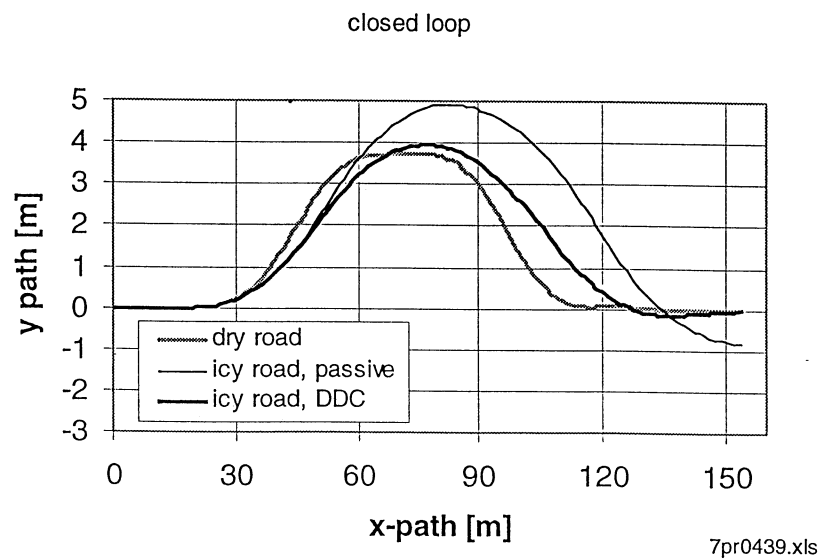


Fig. 18: Double lane change manoeuvre, lateral displacement

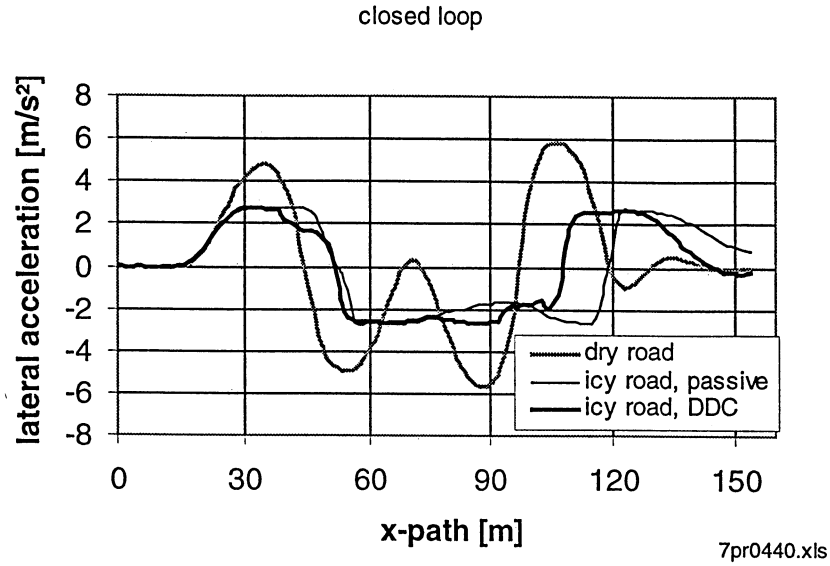


Fig. 19: Double lane change manoeuvre, lateral acceleration

Yaw velocity and side slip angle according to these manoeuvres can be found in the next two figures.

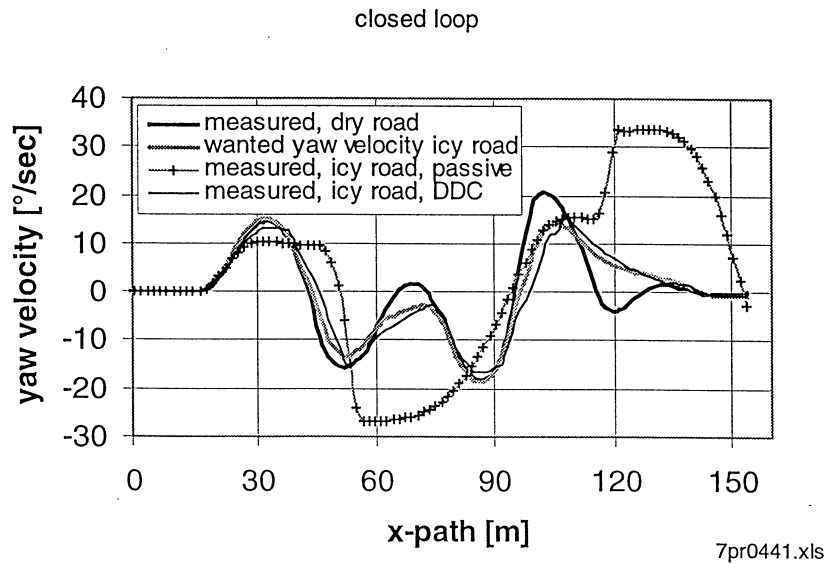


Fig. 20: Double lane change manoeuvre, yaw velocity

The thick black line shows the measured respectively observed values on dry road. The thick grey line shows the wanted values on icy road calculated by means of formula 1 and 2. Among other variables input variable to this formulas is the (controlled) steering angle on icy

road. The controlled yaw velocity reaches the wanted one well. The side slip angle of the controlled vehicle will not exceed 6° which is acceptable (Fig. 21). The side slip angle according to the passive vehicle amounts to 30 degrees (out of diagram range). This manoeuvre is out of control for the average driver.

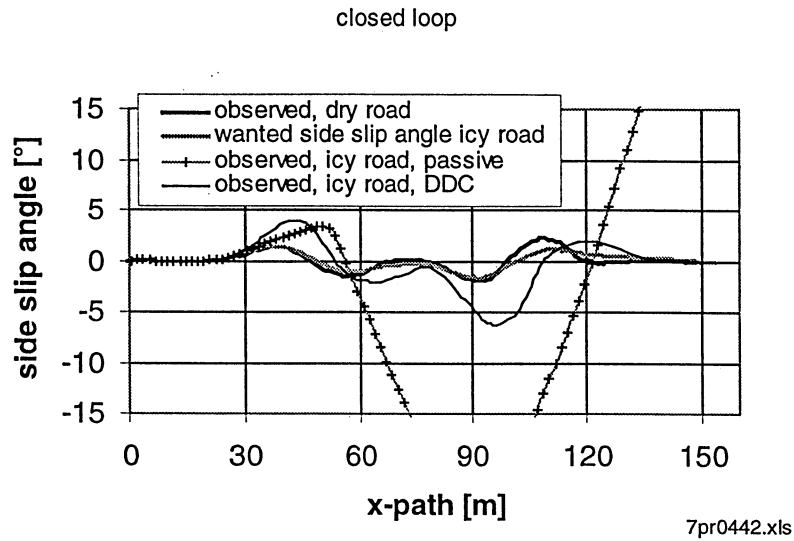


Fig. 21: Double lane change manoeuvre, side slip angle

Fig. 22 shows the adjusted individual brake torque, Fig. 23 shows the resulting longitudinal slip ratios.

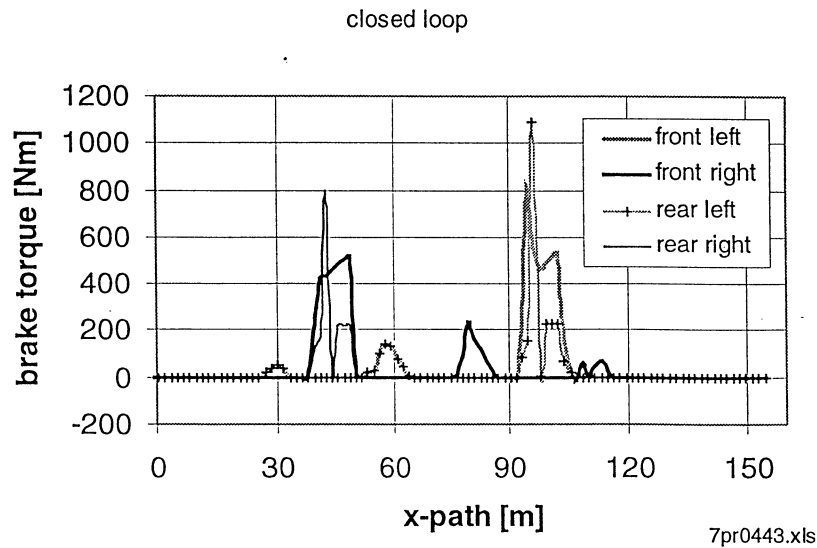


Fig. 22: Double lane change manoeuvre, DDC brake intervention

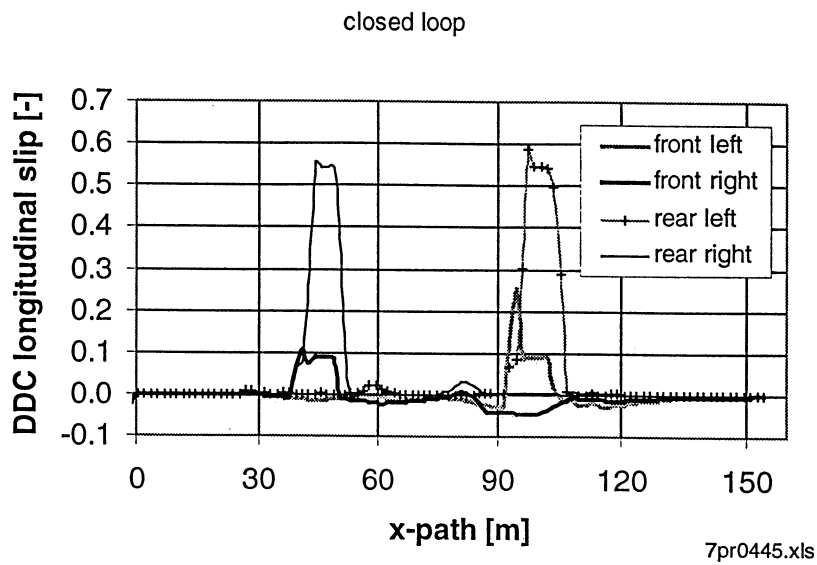


Fig. 23: Double lane change manoeuvre, longitudinal slip ratio

Except for one small part between 90 and 100 meters there is understeering vehicle behaviour. Therefore, the rear slip ratios are up to 0.5, the front ones are less than 0.1. This fact allows higher lateral forces on the front axle being necessary to hold the lane as well as possible

4.3 System errors

By the use of simulation programs like ADAMS and MATRIXx different parameter variations may be handled as fast as influences caused by any system failure. The development can be done under steady environment conditions, dangerous driving tests can be reduced.

This chapter deals with simulations of five different system errors which are:

- system failure at the beginning of the manoeuvre (60 meters)
- system failure in a later manoeuvre state (100 meter)
- offset in the measured yaw velocity (+ 2.5 °/s)
- wrong sign of the measured steering angle
- offset in the observed vehicle velocity (multiplied by 1.5)

The next figures show the steering angle, x-y path, lateral acceleration, yaw velocity and side slip angle according to these errors in comparison to the correctly working system. The manoeuvre is the same double lane change manoeuvre as before.

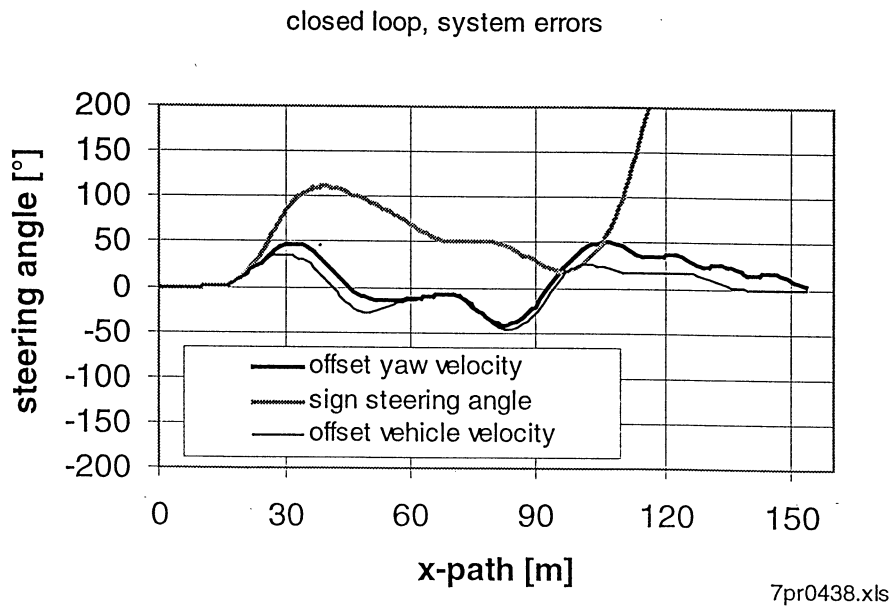
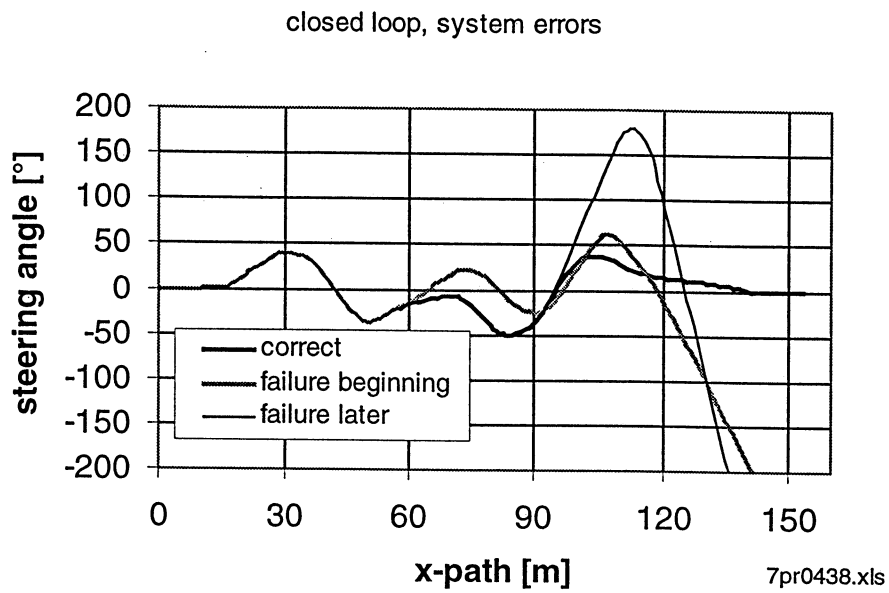


Fig. 24: Simulation of different system failures, steering angle

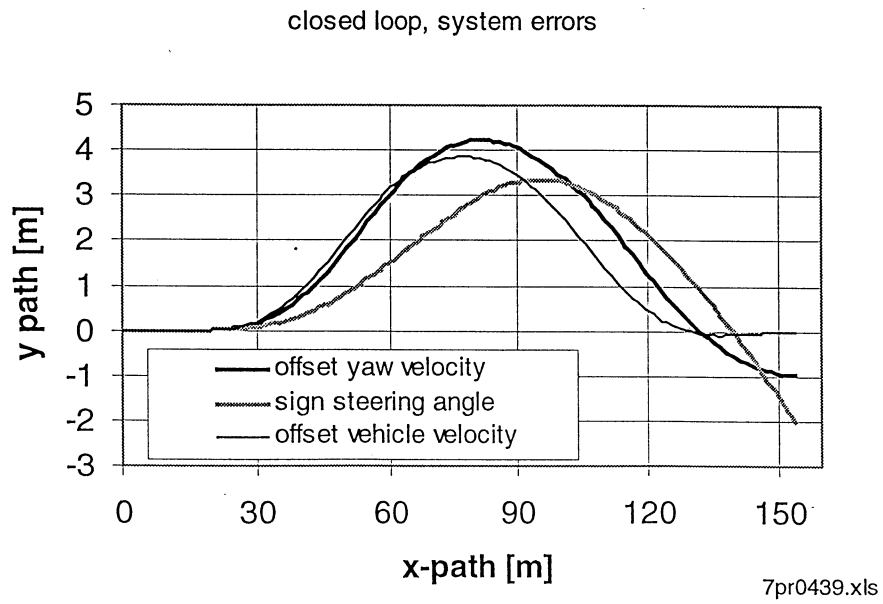
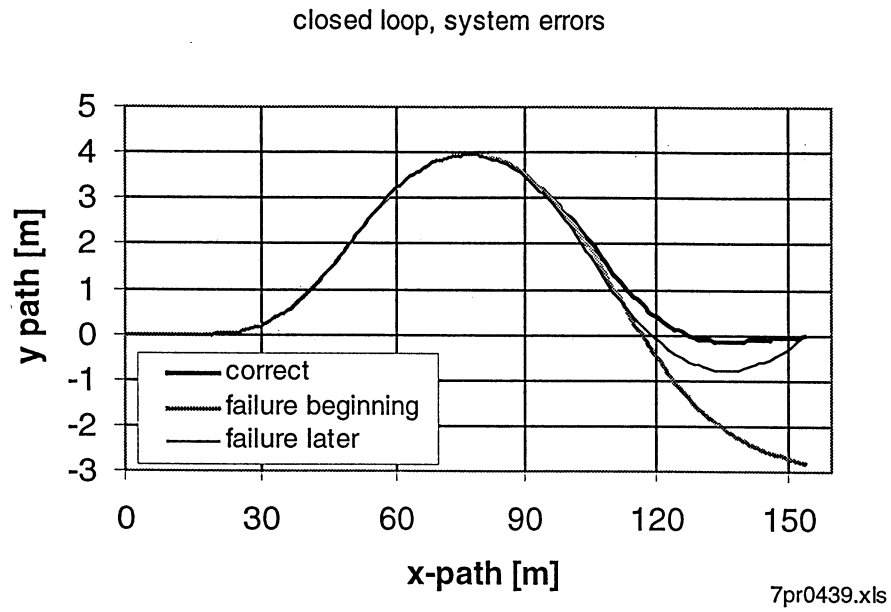


Fig. 25: Simulation of different system failures, x-y path

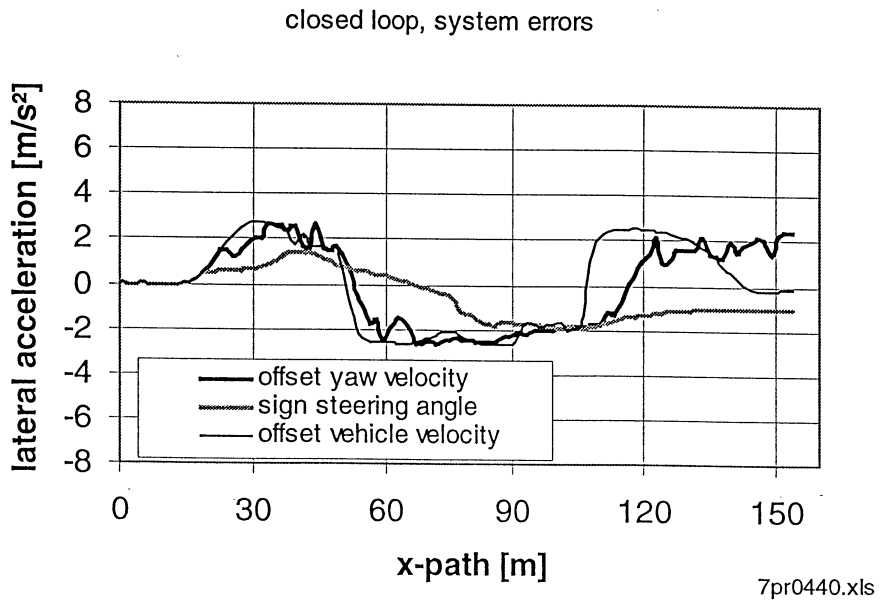
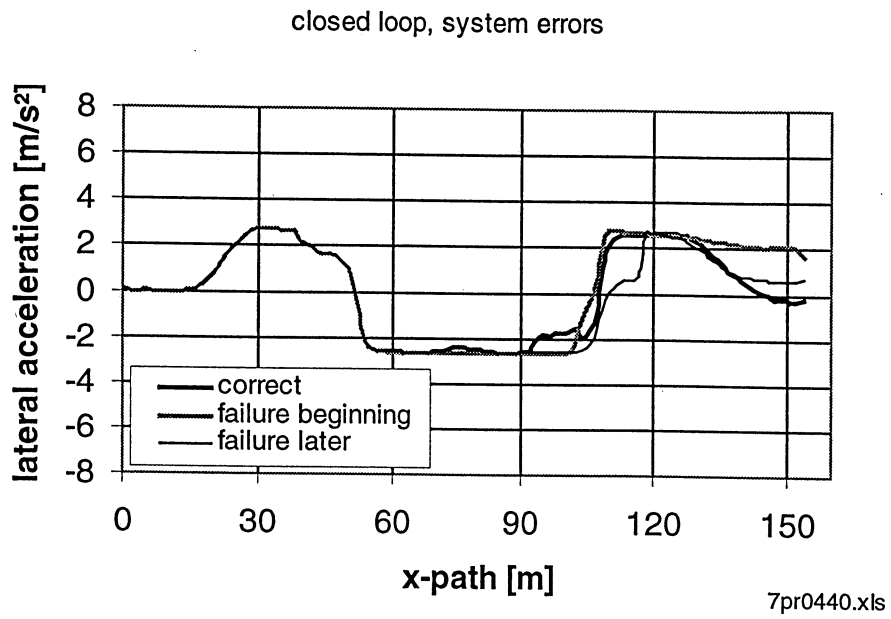


Fig. 26: Simulation of different system failures, lateral acceleration

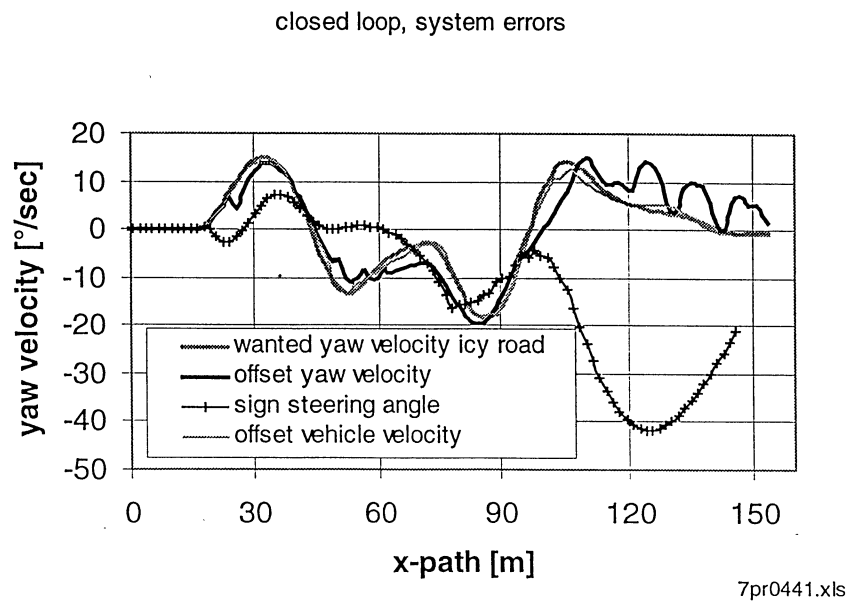
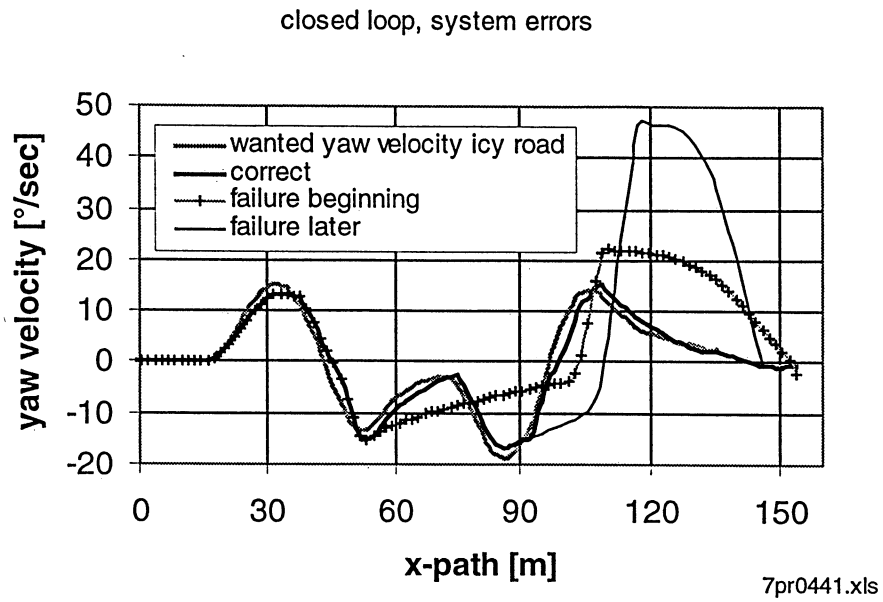


Fig. 27: Simulation of different system failures, yaw velocity

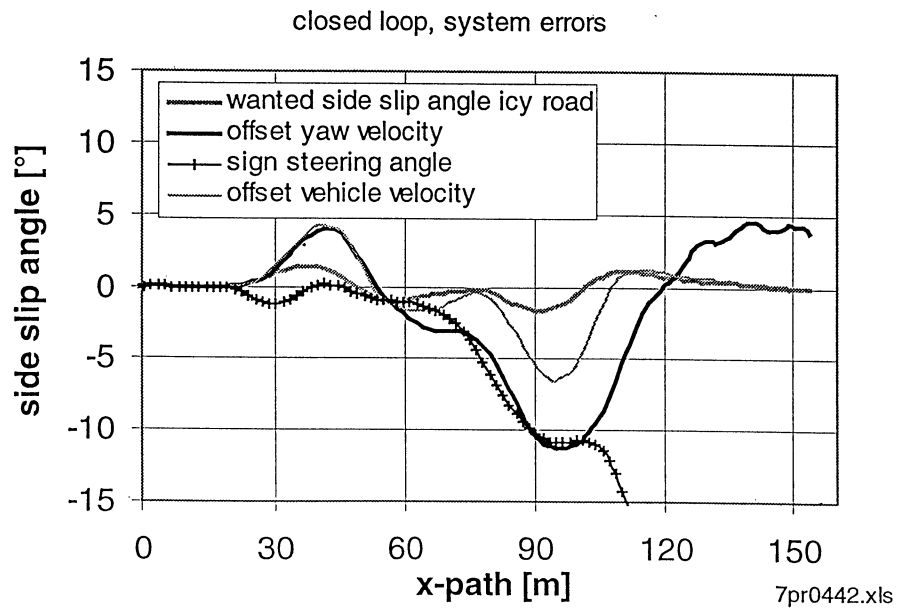
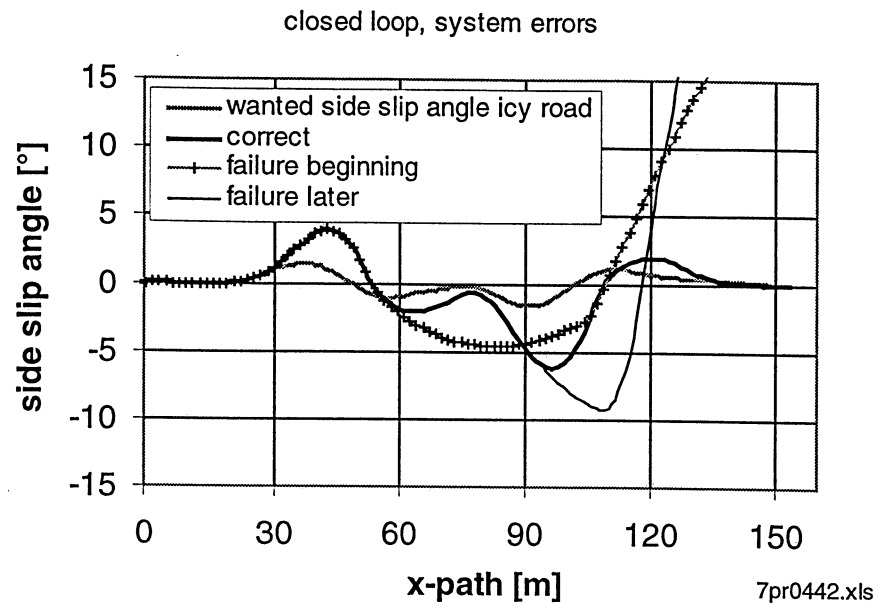


Fig. 28: Simulation of different system failures, side slip angle

The error simulation shows that influences according to system failure at any time during the manoeuvre cause non-stable system reactions. The manoeuvre cannot be handled any longer by the average driver (like the passive vehicle behaviour).

Influences due to offset failure in the vehicle velocity are very small. Offset failures in the measured yaw velocity have greater influences on the driving behaviour. The offset in this example corresponds to the tolerance range which is about ± 2.5 °/s, higher offset errors would cause permanent system intervention. In general, different offset failure effects depend on the offset-size; small offsets can be handled by an average driver.

Wrongly measured steering angle signs cause very dangerous results. The vehicle's behaviour recognised from yaw velocity and side slip angle is quite different from the wanted behaviour. The vehicle cannot even be controlled by good drivers any longer. Non figured simulations with sign mistakes in measured yaw velocity cause the same or even worse results.

5 Conclusion

The combination of both, ADAMS and MATRIXx helps to simulate full vehicle models including integrated controller software. The controller algorithm is generated automatically and can be implemented in real vehicle control systems later on. This procedure allows very fast and flexible development strategies ('rapid prototyping'). The development strategy using ADAMS as hardware model and MATRIXx to develop the control algorithm opens very fast and flexible possibilities. The principal structure of the control strategy can be estimated more accurately than before. In the next time the control algorithm will be implemented in a real prototype vehicle controller and tested under real test track conditions.

The control algorithm in this report has been found exclusively by the use of both software packages, ADAMS and MATRIXx. Therefore, a complex full vehicle model with 81 degrees of freedom and high non-linear tire characteristics has been modelled in ADAMS. Physical processes during driving situations as well as influences of any vehicle or algorithm parameter to the vehicle behaviour can be investigated.

To present the effect of the DDC system, open loop and closed loop driving manoeuvre simulations on snow-covered lane respectively icy road conditions are done. The simulations show that this DDC system is able to use the physical possibilities better than vehicles without controller. The system is working much faster than human response capabilities, the system intervention happens before the driver recognises the dangerous situation.

Of course this system can not help to overcome physical laws. Therefore the driver has to be informed by a warning lamp of any system intervention. But wrong steering inputs by average drivers due to high side slip angles may be reduced as well as dangerous driving situations due to sudden changing road conditions by this Dynamic Driving Control system.

6 References

- [FÖL94] Otto Föllinger, Regelungstechnik, 8. Auflage, Hüthig Verlag Heidelberg 1994
- [KOR94] Willi Kortüm, Peter Lugner, Systemdynamik und Regelung von Fahrzeugen, Springer Verlag Berlin Heidelberg 1994
- [RIC90] Bernd Richter, Schwerpunkte der Fahrzeugdynamik, Verlag TÜV Rheinland GmbH, Köln 1990
- [WAL95] Henning Wallentowitz, Longitudinal Control and Interaction with other Systems, contribution in Smart Vehicles, Swets & Zeitlinger Publishers, Netherlands 1995
- [WAL96] Henning Wallentowitz, Vertikal-/ Ouerdynamik von Kraftfahrzeugen, Umdruck zur Vorlesung Kraftfahrzeuge II, Institut für Kraftfahrwesen Aachen (ika), 1996
- [ZAN96] Anton T. von Zanten et al, Control Aspects of the Bosch-VDC, International Symposium on Advanced Vehicle Control at the Institut für Kraftfahrwesen Aachen (ika), 1996